Mechanistic insights into the directed assembly of hydrogel blocks mediated by polyelectrolytes or microgels

Journal:	*Langmuir*
Manuscript ID	la-2017-00924f
Manuscript Type:	Article
Date Submitted by the Author:	17-Mar-2017
Complete List of Authors:	Hanauer, Nicolas; Universite de Montreal Latreille, Pierre Luc; Universite de Montreal Banquy, Xavier; Universite de Montreal, Faculty of Pharmacy

Mechanistic insights into the directed assembly of hydrogel blocks mediated by polyelectrolytes or microgels

Nicolas Hanauer, Pierre Luc Latreille, Xavier Banquy*

Canada Research Chair in Bio-inspired Materials and Interfaces, Faculty of Pharmacy, Université de Montréal C.P. 6128, succursale Centre Ville, Montréal, QC H3C 3J7, Canada

*corresponding author: xavier.banquy@umontreal.ca

Abstract:

In this study, we report the directed assembly of hydrogel blocks mediated by electrostatic interactions. We compared two different assembly mechanisms, one mediated by microgel particles and another mediated by direct interaction between oppositely charged blocks. The system consisted in hydrogel blocks made of an interpenetrated network of (hydroxyethyl)methacrylate-poly(ethyleneglycol)dimethacrylate (HEMA-PEGDMA) and either positively charged polyethyleneimine (PEI) or negatively charged hyaluronic acid (HA). Positively charged hydrogel blocks were pretreated with negatively charged microgel particles (MG) made of N-isopropylacrylamide-methacrylic acid. Both systems (PEI/HA and PEI/MG) demonstrated spontaneous directed assembly, meaning that positive blocks were systematically found in contact with oppositely charged blocks. Directed assembly in water of PEI/HA blocks resulted in large and open aggregates while PEI/MG blocks exhibited more compact aggregates. Effects of salt and pH were also assessed for both systems. Inhibition of blocks aggregation was found to appear above a critical salt concentration (C^*_{salt}) which was significantly higher for the PEI/HA system (80 mM) compared to the PEI/MG system (5-20mM). The observed difference was interpreted in terms of the nanostructure of the contact area between blocks. Blocks aggregation was also found to be controlled by the content of

negatively charged groups in the microgels as well as the concentration of MG in the suspension (C_{MG}) used to treat the hydrogel block surfaces. Our results shine light on the subtle differences underlying the adhesion mechanisms between hydrogel blocks and suggest new routes toward the design of innovative complex soft materials.

Keywords: hydrogel block, microgels, polyelectrolytes, directed assembly, adhesion

Introduction

Hydrogels, composed of a polymeric matrix and an "immobilized" liquid phase, are ideal materials for bioengineering[1]. On one hand, their polymeric structure is highly versatile and tunable in terms of physical (swelling, stiffness, porosity…) and chemical modifications (functionalizations, sensitivity to environmental cues…). On the other hand, the trapped liquid phase can be used to load and preserve different active compounds (chemical species, growth factors, cells….) in the polymeric network. Since hydrogel matrices are highly tunable, they offer the possibility to design matrices with finely tuned structural environment which in turn can direct the fate of the species they carry [2]. These unique properties have initially been used to develop cargos for drug delivery systems[3, 4]. For example, cell-seeded hydrogel scaffolds with various internal cues are now the prime techniques used for the regeneration of a large variety of tissues (skin [5, 6], cartilage [7, 8], bones[9]…)

Researchers have extensively used assembly techniques to gain a finer control over the microenvironment inside these hydrogel matrices [10]. *In situ* gelation is the easiest path to follow since many different polymeric interactions can lead to the hydrogel formation such as chemical crosslinking[11, 12], electrostatic interactions[13, 14] or complementary binding[15, 16]. In the biomedical field, hydrogel formation is triggered by an external stimulus (temperature, pH…) upon injection of the reactive components. This approach can be limited by physiological conditions, toxicity of the injected components or by the poor control over the hydrogel structure.

An emerging approach to obtain *in situ* hydrogel matrices with controlled architecture is using the directed assembly of prefabricated hydrogel blocks[17, 18]. This bottom-up approach could possibly offer a better control over the three dimensional distribution of embedded active compounds. It might also unlock new possibilities of combining a large spectrum of mechanical and biochemical cues within a defined hydrogel scaffold. This would simply

require selecting formulations and functionalizations needed in separate blocks to design the desired scaffold. It might also be a powerful approach to program a predefined structure to mimic the bio-functional organization of a tissue.

Different experimental techniques have been proposed to facilitate the directed assembly of hydrogel blocks. Blocks aggregation via entropic constraints (such as confinement or concentration increase) can lead to the formation of aggregates but the lack of control over blocks organization and mechanical integrity is still a concern[19]. Microfluidic devices have demonstrated great potential to produce selective aggregation of a few blocks but their ability to produce large scale tissues-sized, aggregates seems more difficult to adapt[20, 21, 22]. Stabilization of blocks in water-in-oil droplets followed by secondary photo crosslinking has allowed a fine control over the size of the blocks aggregates but not over their final internal structure[23]. Using templates with hydrophobic and hydrophilic regions is also a method to guide blocks organization on a patterned surface[24] but appears to be challenging to translate into 3D structures. Tissue printing is certainly the most promising solution towards 3D organization of cell-laden hydrogels is extensively used to obtain layered materials rather than injectable blocks[25]. Other fabrication techniques have also been proposed via the incorporation of magnetic cues to guide the blocks assembly[26].

Nevertheless, since hydrogels are easily tunable, the most promising approach to obtain scaffolds with programmable internal structures is based on block-block interactions, especially to promote directed assembly. Hydrogel blocks can be designed to interact and adhere specifically with neighboring blocks. A wide spectrum of adhesive mechanisms have been tested for that purpose: Michael type addition between reactive groups at blocks surfaces[27], molecular recognition via host-guest interactions[28, 29], complementary DNA chains incorporated in the hydrogel blocks[30], nucleation and growth of collagen fibers at interfaces [31]. These techniques make use of a wide variety of adhesion mechanisms, resulting in

complex, structurally controlled hydrogel assemblies. Furthermore, it has been demonstrated that surface modification with polymers brushes or nanoparticles can also efficiently promote adhesion between soft surfaces[32, 33, 34, 35]. Besides the large body of work demonstrating the potential uses of structurally programmed matrices, there is a lack of systematic studies comparing their assembly mechanism and sensitivity to external physical factors. Such knowledge is critical to promote the development of more complex materials integrating a large number of chemical, structural and physical characteristics.

In this report, we have intended to rationalize the assembly of hydrogel blocks mediated by electrostatic interactions. We studied two different interaction mechanisms, one where hydrogel blocks assembly is mediated by direct contact between oppositely charged blocks and a second mechanism where assembly between identical blocks is mediated by oppositely charged microgel particles (MG). The hydrogel blocks were fabricated by UV photolithography in presence of different polyelectrolytes (PEI or HA). Since electrostatic forces were expected to drive the blocks assembly, we studied the effect of pH, ionic strength and microgel composition to elucidate differences between the two interaction mechanisms.

Materials and methods:

Materials

2-hydroxyethyl methacrylate (HEMA, 97%), poly(ethylene glycol)dimethacrylate (PEGDMA, Mn = 550g/mol), N,N′-methylenebis(acrylamide) (BisA, 99%), N-Isopropylacrylamide (NIPAM, >99%), sodium dodecyl sulfate (SDS, >98.5%), methacrylic acid (MAA, 99%) hydrochloric acid (HCl, 37%) and aluminum oxide (activate, basic, Brockmann I) were purchased from Sigma-Aldrich Canada, Ltd. (Oakville, Canada). Irgacure 2959 was a kind gift from BASF (Mississauga, Canada). Polyethyleneimine (PEI, branched, Mw = 10 000g/mol, 99% purity) was from Alfa Aesar (Ward Hill, USA). Sodium hyaluronate

(HA, Mw = 60 000 g/mol) was purchased from LifeCore Biomedical (Chaska, USA). Sodium chloride (NaCl) and ammonium persulfate (APS) were from Fisher Chemical (Ottawa, Canada). Unless stated, materials were used without prior purification.

Hydrogel blocks preparation

Blank hydrogel blocks were obtained via photopolymerization of HEMA using PEGDMA as a cross-linker. After purification on a basic aluminum oxide column, a mixture of HEMA-PEGDMA (99.8:0.2 mol%) was dissolved in water (65 wt%) for 10 min under magnetic stirring. Irgacure 2959 was then added as photoinitiator (5 wt% total). The mixture was then placed under high intensity UV lamp (UVP Mercury Spot Low, 100MW Longwave) for 30 min.

Hydrogel solutions were injected in a mold composed of two glass slides separated by a glass spacer. The loaded mold was then covered with a photomask and another glass slide. The photomasks consisted of a transparent slide imprinted with the periodic arrangement of the blocks shape. With this technique, we were able to obtain hydrogel blocks of size larger than 1mm and thickness ranging between 0.15mm to 3mm depending on the thickness of the spacer used. After polymerization, the injection mold was opened, the unreacted mixture was washed away with water under pressure and the blocks were gently separated from the glass plates with a spatula. Blocks were then kept in water (~25 blocks / 10mL) under high magnetic stirring to ensure complete swelling and removal of unreacted monomers.

Positively charged hydrogel blocks were obtained by adding polycationic PEI (25 wt%) prior to the photopolymerization step. PEI was added to the HEMA-PEGDMA mixture and then dissolved in water at around 40°C, allowing for the complete dissolution of PEI. PEI blocks were colored in red by adding a few droplets of a Rhodamine 6G solution (0.5mg/mL) in the monomer mixture before polymerization. Similarly, in order to obtain negatively charged blocks, an anionic polyelectrolyte was added to the reagents mixture prior to

photopolymerization. A HA solution (3mg/mL) was prepared one day prior to photopolymerization in a water and HCl mixture (6.6 vol%). This HA solution was used to mix the monomer solution of HEMA and PEG-DMA at a final concentration of 35 wt%. HA blocks were colored in blue using a food coloring dye before polymerization.

The second procedure used to produce negatively charged blocks was to treat positively charged blocks with a solution of negatively charged NIPAM-MAA microgels. Blocks were immersed in a MG solution at C_{MG}= 4mg/mL (25 blocks/10mL, 24 hours) under magnetic stirring and then rinsed in water for 1 hour to eliminate non adsorbed microgels.

Microgels synthesis

NIPAM-MAA microgels used in this study were synthesized by precipitation polymerization. Briefly, monomers (NIPAM with MAA at 0, 5, 10 or 20 mol%), BisA as cross-linker (5mol% total monomers) and SDS (867µmol/L) as surfactant were dissolved in degassed water. The mixture was then placed at 65°C under mechanical stirring (200 rpm) and argon atmosphere for equilibration. APS (2.9 mmol/L) was then injected in the reaction vessel. Polymerization was let to proceed during 4h30 at a temperature of 75°C and constant stirring of 300 rpm. The resulting particle solution was then dialyzed (Spectra/Por Tube-A-Lyzer Dynamic Dialysis Device, 100 kDa MWCO) against milliQ water (~60mL of particle suspension for 20L of water, overnight). Four batches of microgels were synthesized containing 0 to 20 % of MAA. The concentration of microgels, C_{MG}, in the final suspension was determined by lyophilizing a volume of 1.5 mL of suspension. Size, polydispersity and ζ potential of the MG particles (100-800µg/mL) in water and in presence of different salt concentrations at 22°C were characterized via dynamic and phase analysis light scatterings (DLS and PALS) using a Brookhaven NanoBrook Omni (90° detection angle, illumination wavelength 640nm). The microgels zeta potential was found to be negative independently of the MAA content. Since the polymerization of NIPAM was initiated by ammonium persulfate which is negatively

charged in solution, the polymer chain ends bearing the initiator moiety are expected to provide negative charges at the surface of the microgel even at 0% of MAA.

Directed assembly tests

Tests were performed in small crystallizers filled with 10 mLof distilled water. Mixtures of positively and negatively charged 2x2x1mm^3 blocks were suspended together under constant mixing conditions with an orbital shaker (150-200 RPM, 3min) until completion of the assembly process. Upon completion of the assembly process, aggregates were imaged and counted under a stereoscopic microscope (Zeiss Stereo Discovery V8 stereomicroscope). Each assembly test was carried out in quintuplet and data were reported as mean value ± standard deviation. Cycles of assembly and disassembly were performed during each test to evaluate surface integrity and directed assembly reproducibility. Once an aggregation test was performed, the cubes were gently separated using a spatula before repeating next assembly test. When the adhesion between the cubes was weak, gentle manipulation without inserting the spatula in between the cubes was sufficient to separate them.

The effects of C_{salt} and pH on the aggregation process were also studied. Salinity of the media was controlled using NaCl. Blocks were left 10 min or 24h to equilibrate in a NaCl solution (25 blocks/10mL) before testing their assembly in freshly prepared saline medium. Assembly tests under acidic or basic conditions were achieved using a similar protocol with HCl and NaOH solutions (pH =3 and 10.5, 24h equilibrium). Imaging of the blocks and aggregates was performed on a Zeiss Stereo Discovery V8 stereomicroscope under high illumination. During observation, the samples were immersed in water in a small crystallizer.

Results

For both types of systems, i.e. oppositely charged blocks (PEI/HA) or blocks pretreated with microgels (PEI/MG), we were able to observe the directed assembly of the hydrogel blocks, meaning that we obtained aggregates able to resist gentle spatula manipulation (see Figure 1). Even if we observed the blocks assembly for both systems, macroscopic observations of the aggregates seemed to demonstrate that two types of adhesion mechanisms were involved. PEI/HA aggregates were indeed larger in size and deformable under gentle manipulation or agitation compared to the more compact PEI/MG aggregates (see Figure 1D and H for examples of large and compact aggregates). These differences in aggregate structure were more pronounced for larger size aggregates (Figure 1Dand H) compared to smaller size aggregates (Figure 1B and F). Control experiments with single block populations (HA/HA, PEI/PEI or PEI/MG-PEI/MG) did not lead to any directed assembly. Moreover, control tests using HA, PEI and PEI-MG blocks with neutral HEMA-PEGDMA hydrogel blocks did not lead to any aggregate formation as well.

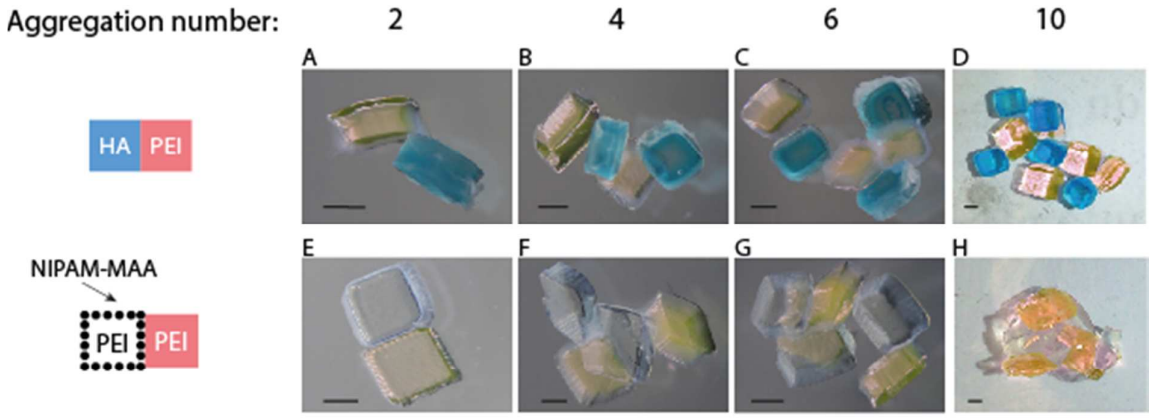

Figure 1: Microscopy images of PEI/HA (A-D) and PEI/MG (E-H) aggregates of different sizes (scale bar: 1mm) obtained after completion of the aggregation process.

Both studied systems were tested under different conditions to investigate their properties and differences. In a first series of test, we studied the effect of the population size for the PEI/HA system, i.e. the effect of blocks concentration on aggregates size (maintaining the ratio between block partners equal to 1). We studied three PEI/HA blocks populations: 3:3, 5:5 and 10:10 by performing 5 iterations of the aggregation test with the same blocks. For the three tested populations, the average aggregates size was significantly reduced after the first aggregation test and continued to gradually decrease until 5 iterations were performed (See Figure 2).

We observed that an increase of the block population size led to larger aggregates at the first iteration (the cumulative percentage reaches 100% at a high aggregation number). For example, the 10:10 population exhibited large aggregates only (> 17 blocks) after the first aggregation test while the 3:3 and 5:5 populations lead to a mixture of mid-sized aggregates (4 to 6 blocks per aggregates).

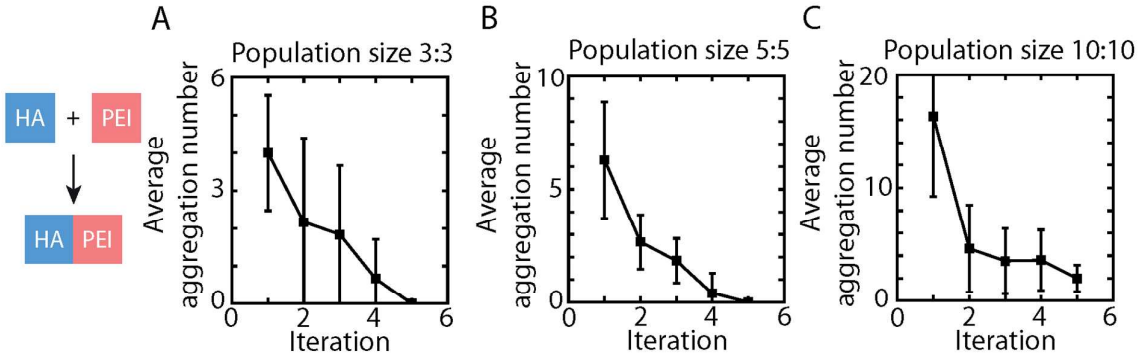

Figure 2: Average aggregation number as a function of the experiment iteration for different blocks concentrations. Error bars represent the standard deviation of 5 separate experiments.

In the next series of experiments, we compared the aggregation processes of our two systems. For the PEI/MG system, PEI blocks pretreated with MG were mixed with equal number of untreated PEI blocks. We tested 4 types of MG containing increasing amount of MAA (See Table 1) and studied the directed assembly of the hydrogel blocks after pretreatment with these microgels (C_{MG} = 4mg/mL, 25 blocks / 10mL, 24 hours). We used a block population

size of 5:5 and performed 3 consecutive assembly/disassembly iterations for each test (see Figure 3).

We observe that, while pretreatment with microgels containing MAA 0% did not lead to any aggregation, pretreatments with the three other types of microgels (MAA 5%, 10% and 20%) lead to the formation of large aggregates at the first iteration (with 8 to 10 blocks per aggregate). Increasing the number of assembly/disassembly cycles slightly decreased the aggregates size but did not inhibit their formation in contrast to our previous observations with the PEI/HA blocks.

Table 1: Particle size and ζ-potential of the NIPAM-MAA microgels

MAA%	d (nm)	ζ-potential (mV)
0%	211.6±1.4	-14,3±0,9
5%	303.1±2.8	-23,8±1,1
10%	375.0±3.8	-27,2±0,8
20%	557.1±4.4	-29,3±1,3

In Figure 3, the pretreatments of the PEI blocks with the MG were conducted at C_{MG}= 4mg/mL which we supposed was above the concentration necessary to reach saturation of the block surfaces. To confirm this hypothesis, we tested different pretreatments concentrations, for all the MG (MAA 5%, 10% and 20%) ranging from C_{MG} = 0.008mg/mL to 8mg/mL. In Figure 4A, the total aggregation % (the total percentage of aggregated blocks independently of the aggregate size) is represented versus the MAA concentration in the microgel suspension during pretreatment (C_{MAA}) after one aggregation experiment (5 separate repetitions). We observed that aggregation of the hydrogel blocks did not occur below a critical concentration, C^*_{MAA}, which increased with the MAA content in the microgels, from 2.9 µg/mL for MAA 5% to 11.7µg/mL for MAA 20%. Interestingly, these values of C^*_{MAA} corresponded to a similar microgel concentration, C^*_{MG} = 0.04 mg/mL for all the MG.

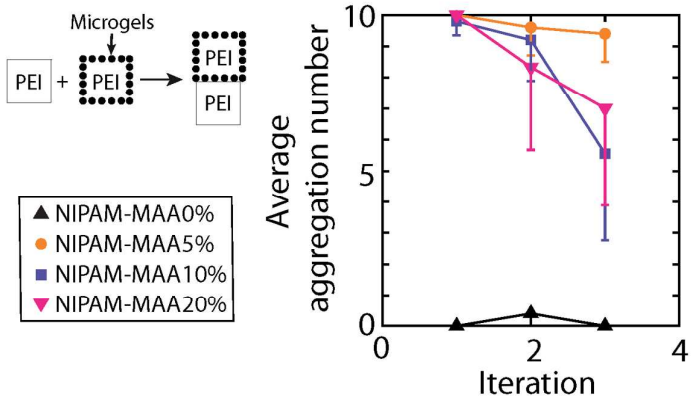

Figure 3: Effect of MAA content in microgels on the directed assembly of PEI-containing hydrogel blocks. In contrast to the data shown in Figure 2, the average aggregation number of this system only slightly decreases with the number of assembly/disassembly iteration. Error bars represent the standard deviation of 5 separate experiments. Curves are guides for the eye.

One possible explanation of such behavior is that the microgel size increases significantly with the MAA content (Table 1) without any significant changes in zeta potential. Therefore, most of the MAA is expected to be located inside the microgel particle and not at its surface. Consequently, the charge surface density is expected to decrease with the MAA% in the microgel which could explain why C_{MAA}* was found to increase with MAA%.

In Figure 4B-D, we show the evolution of the average aggregation number as a function of the assembly/disassembly iteration number for each microgel concentration used. In these panels, the indicated concentration of microgels corresponds to the microgel concentration in the pretreatment suspension. Results show a quasi-constant (or slightly decreasing) average aggregation number for C_{MG} > 0,08mg/mL and complete loss of blocks aggregation when C_{MG} < 0.08 mg/mL. Results were identical for MAA5%, 10% and 20% microgel pretreatments. We also noticed that pretreatment with the MAA 20% microgels at 0.08mg/mL systematically lead to significantly smaller aggregates compared to the other MG at the same C_{MG}. Observation of a similar aggregate distribution and average aggregation number at C_{MG} superior to 0.08mg/ml, independently of the MAA content in the microgels, tends to confirm that the saturation of the hydrogel blocks surfaces was reached at these MG

concentrations. In Supplementary information 3, the evolution of the cumulative percentage of aggregated cubes as a function of the aggregation number confirmed that the size distribution of the aggregates was not affected at C_{MG} > 0.08 mg/mL.

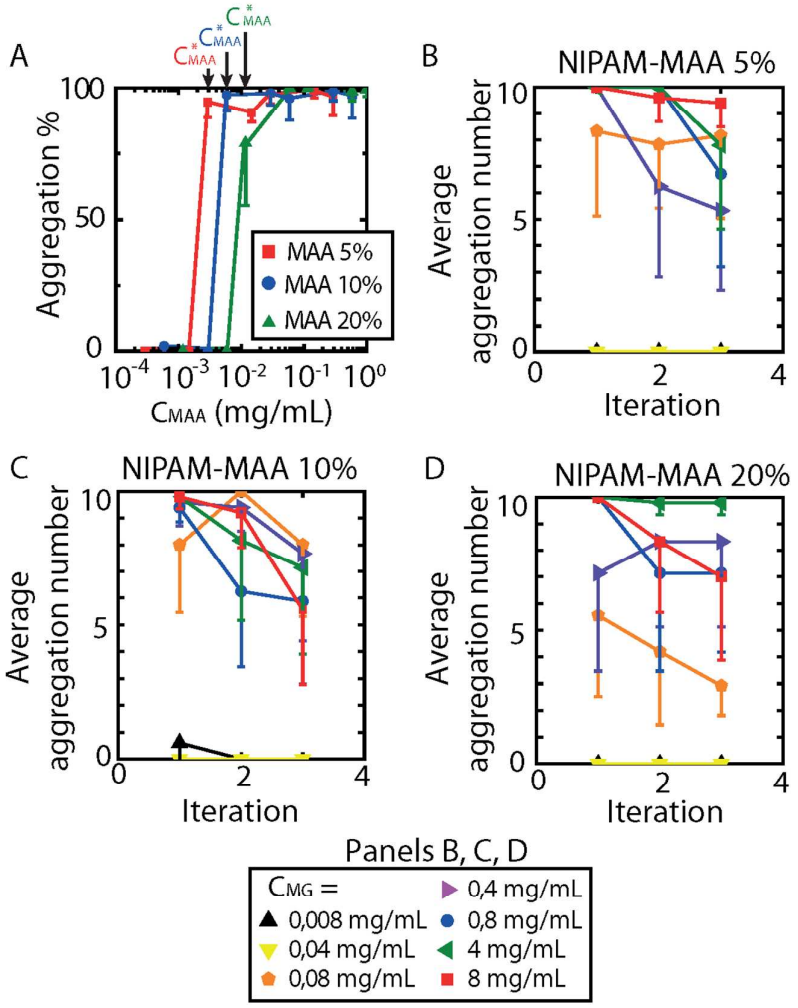

Figure 4: Effect of microgel concentration on the directed assembly of PEI blocks. A) Blocks aggregation % as a function of the MAA content in the microgels during the pretreatment. B-D) Average blocks aggregation number as a function of the experiment iteration. Error bars represent the standard deviation of 5 separate experiments. Lines are guides for the eye.

To understand the role played by the electrostatic forces in the assembly of the hydrogel blocks, we performed a series of aggregation tests at increasing salt concentrations (C_{Salt}= 0-150mM NaCl, see Figure 5A). Above a critical salt concentration,C^*_{Salt}, the aggregation of the

hydrogel blocks was strongly hampered, independently of the system. PEI/HA aggregates were found to resist significantly more to the increase in salinity (C^*_{Salt}= 80 mM), even after prolonged incubation in saline solution (24h) compared to PEI/MG systems. The value of C^*_{Salt} was found to depend on the MG composition, and increased with the MAA content, from C^*_{Salt} = 5mM for MAA 5% to C^*_{Salt} = 20mM for MAA 20%. The value of C^*_{Salt} was also found to depend on the C_{MG} (See Figure 5B). While the pretreatments with C_{MG} = 8 and 4mg/mL presented similar behavior (C^*_{Salt}=20mM), a decrease in C^*_{Salt} was observed at C_{MG} = 0.4mg/mL (C^*_{Salt}= 10mM) until almost complete loss of directed assembly was observed at C_{MG} = 0.08mg/mL (C^*_{Salt}= 2.5mM).

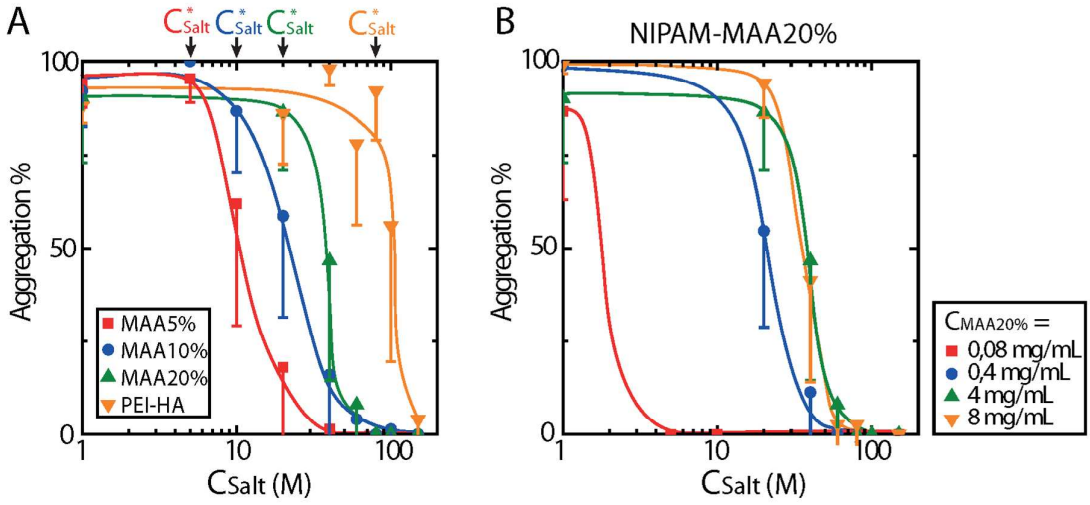

Figure 5: Effect of salt concentration on the directed assembly of A) PEI/HA and PEI/MG systems B) PEI/MG system in presence of microgels NIPAM-MAA20% at different concentrations. Lines are guides for the eye.

Since the two systems under study are composed of pH-sensitive materials (PEI and HA), the effect of pH on the directed assembly of the hydrogel blocks was also studied. We compared our previous results obtained in pure water (pH = 6) with tests performed in acidic (pH = 3) and basic (pH = 10.5) conditions (see Figure 6). Results show a complete loss of assembly at a pH above or below pH = 6 after 24h of equilibrium.

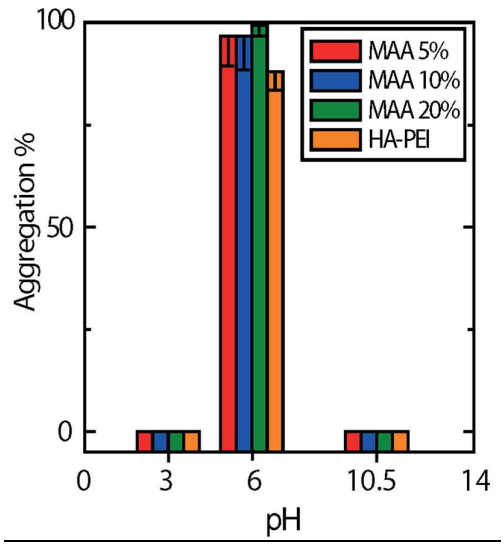

Figure 6: Effect of pH on the directed assembly (aggregation) of PEI/HA and PEI/MG systems

Discussion

Macroscopic observations of the blocks aggregates pointed out differences in interaction strength between PEI/HA and PEI/MG systems. Larger PEI/HA aggregates were indeed systematically observed compared to more compact PEI/MG aggregates. For the PEI/HA system, we observed that the blocks concentration (population size) played an important role in determining the aggregates size, which means that every random contact between positive and negative blocks did not necessarily lead to an adhesive contact. Nevertheless, only adhesive contacts between positive and negative blocks were observed, demonstrating that directed assembly, in opposition to self-assembly, was effectively happening. The total loss of assembly capacity of the PEI/HA blocks after a few iterations strongly suggest that the hydrogel blocks surfaces are very sensitive to mechanical manipulation and therefore prone to damage. Surface damage can occur in the form of surface roughening or material transfer between surfaces (which leads to surface charge compensation), both causes leading to adhesion loss and consequently to a decrease of the aggregation number. Those initials observations suggested that in the case of the PEI/HA system, adhesive contacts are mostly

promoted by steric entanglements and electrostatic interactions between polyelectrolytes chains present at the hydrogel blocks surfaces (See Figure 7A).

We observed that the effect of C_{Salt} on the blocks aggregation is not gradual, meaning that the aggregates size did not continuously decrease with salt concentration. Instead, an abrupt transition from an aggregated to a disaggregated state was observed around C^*_{Salt}. Surprisingly, C^*_{Salt} was found to be much higher for the HA/PEI system compared to the PEI/MG system suggesting that other than purely electrostatic forces might be at work in this system. In fact, the large variability in the assembly process of HA-PEI blocks and the high C^*_{Salt} value indicate that electrostatic and macromolecular entanglements are involved in the adhesion mechanism.

Since HA and PEI are polyelectrolytes, their ionization degree is directly determined by the pH of the medium. HA possess carboxylic acid groups with a pKa ≈ 3-4[36]. While HA chains are only partially negatively charged at pH = 3 (24% ionization, pH ≈ pKa), at pH = 6 and 10 HA is fully neutralized (pH >pKa). On the other hand, branched PEI possess primary, secondary and tertiary amines and therefore three respective pKa (4.5, 6.7 and 11.6 [37]). Using the structure of the branched PEI used in this study (primary:secondary:tertiary amines ratio of 4:3:4), the total amount of ionized amine groups (in form of NH^+, NH_2^+ and NH_3^+) available on the PEI chains at a given pH can be estimated. At pH = 3, 98.9% of the amine groups are positively charged, 60.2% at pH =6 (secondary and tertiary amines) and only 33.7% at pH = 10.5 (tertiary amines only). To insure rapid adhesive electrostatic interactions between block surfaces, negative and positive surfaces must be significantly ionized. This explained why assembly was only observed at pH =6. At this pH, blocks exposed significant amount of charged groups (99.7% for HA and 60.2% for PEI), which was not the case at pH = 3 (24% HA ionization) and 10.5 (33.7% PEI ionization). Moreover, polyelectrolyte charge has an effect on chains conformation. At high ionization degree, polymer chains from one

block's surface are expected to expand which favors overlapping and entanglement upon contact with another surface and therefore adhesion. Our study shows that assembly of hydrogel blocks can occur at partial ionization of the polyelectrolytes (60% for PEI) but can be inhibited if ionization is too small (the minimum being located between 30 and 60%).

As for the PEI/MG systems, MGs were found to act as efficient adhesion promoters between positively charged blocks. By electrostatically interacting with the PEI chains and potentially the network of HEMA-PEGDMA forming the blocks, MGs can create a negatively charged layer at the block surfaces which favors electrostatic bridging with PEI chains (See Figure 7B). Since the MGs are significantly more crosslinked than the hydrogel blocks, interpenetration between polyelectrolytes chains and MGs is expected to be disfavored. Therefore, microgel adsorption and blocks adhesion are both driven by MAA groups at the surface of the microgel. This explanation is also confirmed by the fact that no directed assembly with MGs of pure NIPAM (which were found to be slightly charged) was observed.

One major difference between the PEI/MG and the PEI/HA systems is the surprisingly good assembly reproducibility after several iterations of the PEI/MG system (See Figure 3). The most straightforward explanation of this observation is the absence of damage under mechanical manipulation of the blocks, and a perfectly reversible interactions between PEI blocks and MGs. This would suggest that MGs adsorbed at the blocks surfaces are compliant and can easily move on the gel interface to adapt their conformation and avoid surface damage.

The effect of the ionic strength seems to be modulated by the composition of the microgels. The critical concentration at which assembly was inhibited, C^*_{Salt}, was found to increase strongly with the MAA% in the microgels from 5 mM for MAA 5% to 20 mM for MAA 20%. This observation confirms the crucial role of MAA moieties on the interactions between block surfaces. The disrupting effect of NaCl is explained by the hindering of the interactions

between MAA at microgel surfaces and PEI chains (See Figure 5A). Higher MAA content in the MGs explain the increased C^*_{Salt} as more chloride anions are needed to completely screen PEI-microgels interactions. Stability tests also confirmed that microgels were stable at very high C_{Salt} (data not shown). The critical coagulation concentrations of the microgels are indeed significantly higher than the C_{Salt} used in our tests meaning that the microgels remained as a stable colloidal suspension and, at least in part, electrostatically charged and thus prone to interactions with PEI chains. Loss of directed assembly could also be due to PEI polyelectrolytes chains reorganization and folding, decreasing possible interactions with the MGs.

The influence of pH on the directed assembly of PEI/MG is quite similar to PEI/HA system. Linear MAA chains with a degree of polymerization superior to 20, present a pKa of 6.5[39]. Considering this information, microgels should exhibit no ionization of the MAA at pH=3 and complete ionization at pH = 10.5 (>99.9%). Therefore, in acidic or basic conditions, MAA and PEI are not ionized enough to favor electrostatic interactions. At pH = 6, MAA presents 24.0% of ionization which seems sufficient to promote interactions with the charged amines of the PEI. However, the fate of the microgels after PEI/MG block equilibrations at pH = 3 and 10.5 solutions remains unknown. It is indeed unclear if microgels remained adsorbed or entrapped in the HEMA-PEDGMA and PEI networks or if they were released upon loss of ionization.

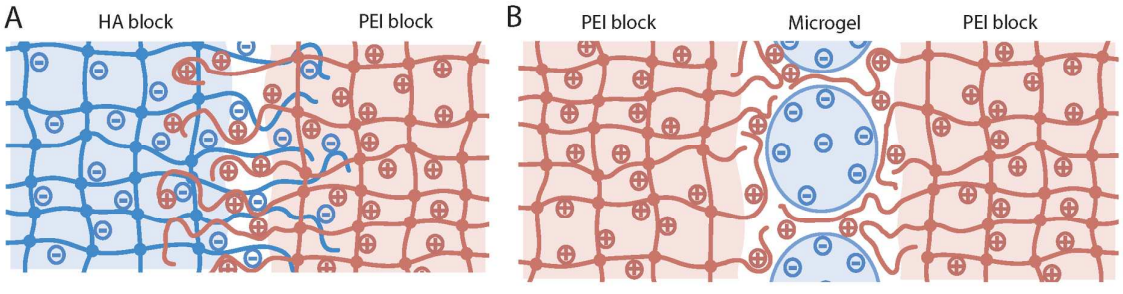

Figure 7: Models of supposed interactions at hydrogel blocks surfaces during adhesive contacts, A: steric entanglement guided by electrostatic cues between HA and PEI

polyelectrolytes chains, B: bridging between PEI chains and NIPAM-MAA microgels without any entanglements involved.

In summary, the assembly of PEI/HA blocks were found to be driven by electrostatic interactions and steric entanglements. As a consequence, this system was prone to surface damage upon repeated forced desaggregation. The PEI/MG system is based on the reversible electrostatic interactions between ionized MAA groups in the MGs and PEI polyelectrolytes chains. This systems was not damaged under mechanical manipulation but was highly sensitive to ionic strength. These observations highlight the important, and overlooked role of the interface microstructure in the adhesion mechanism (see Figure 7). Hydrogel-hydrogel interfaces in presence of microgels are expected to be rougher compared to direct hydrogel-hydrogel contacts allowing for ions to quickly penetrate the interface and to destabilize it even if the adhesive strength between blocks is stronger.

Conclusions

This study presents the directed assembly of charged hydrogel blocks mediated by microgel particles or by direct contact. In both systems studied, random contacts between blocks resulted in the formation of aggregates. PEI/HA directed assembly in water resulted in large, flexible aggregates vulnerable to mechanical manipulation, while PEI/MG aggregates were more compact and resistant. Such difference was attributed to a difference in adhesion strength between blocks. The PEI/MG system presented the highest sensitivity to ionic strength, highlighting the role of the interface microstructure and porosity in the adhesion phenomena.

These results provide new insights into the adhesion mechanism between soft materials in presence of a third body such as microgels, proteins or solid nanoparticles and should guide the development of future materials with controlled tunable properties.

Acknowledgements

XB is grateful for the financial support of FRQ-NT (new researcher program) and CRC. NH acknowledges the financial support of the Faculty of Pharmacy (recruitment scholarship). PLL is grateful for financial support of GRUM, Faculty of Pharmacy, FRQ-NT and NSERC.

References

1. Hoffman, A. S. Hydrogels for biomedical applications. *Adv. Drug Del. Rev.* **2012,***64, Supplement*, 18-23.
2. King, W. J.; Krebsbach, P. H. Growth factor delivery: How surface interactions modulate release in vitro and in vivo. *Adv. Drug Del. Rev.* **2012,***64* (12), 1239-1256.
3. Hanauer, N.; Latreille, P.; Alsharif, S.; Banquy, X. 2D, 3D and 4D Active Compound Delivery in Tissue Engineering and Regenerative Medicine. *Curr. Pharm. Des.* **2015**.
4. Hoare, T. R.; Kohane, D. S. Hydrogels in drug delivery: progress and challenges. *Polymer* **2008,***49* (8), 1993-2007.
5. Priya, S. G.; Jungvid, H.; Kumar, A. Skin tissue engineering for tissue repair and regeneration. *Tissue Eng. Pt B-Rev* **2008,***14* (1), 105-118.
6. Metcalfe, A. D.; Ferguson, M. W. J. Bioengineering skin using mechanisms of regeneration and repair. *Biomaterials* **2007,***28* (34), 5100-5113.
7. Lam, J.; Clark, E. C.; Fong, E. L. S.; Lee, E. J.; Lu, S.; Tabata, Y.; Mikos, A. G. Evaluation of cell-laden polyelectrolyte hydrogels incorporating poly(l-Lysine) for applications in cartilage tissue engineering. *Biomaterials* **2016,***83*, 332-346.
8. Muzzarelli, R. A. A.; Greco, F.; Busilacchi, A.; Sollazzo, V.; Gigante, A. Chitosan, hyaluronan and chondroitin sulfate in tissue engineering for cartilage regeneration: A review. *Carbohydrate Polymers* **2012,***89* (3), 723-739.
9. Griffin, K. S.; Davis, K. M.; McKinley, T. O.; Anglen, J. O.; Chu, T.-M. G.; Boerckel, J. D.; Kacena, M. A. Evolution of Bone Grafting: Bone Grafts and Tissue Engineering Strategies for Vascularized Bone Regeneration. *Clin. Rev. Bone. Miner. Metab.* **2015,***13* (4), 232-244.
10. Yang, J.-A.; Yeom, J.; Hwang, B. W.; Hoffman, A. S.; Hahn, S. K. In situ-forming injectable hydrogels for regenerative medicine. *Prog. Polym. Sci.* **2014,***39* (12), 1973-1986.
11. Shu, X. Z.; Liu, Y.; Palumbo, F. S.; Luo, Y.; Prestwich, G. D. In situ crosslinkable hyaluronan hydrogels for tissue engineering. *Biomaterials* **2004,***25* (7), 1339-1348.
12. Cai, S.; Liu, Y.; Shu, X. Z.; Prestwich, G. D. Injectable glycosaminoglycan hydrogels for controlled release of human basic fibroblast growth factor. *Biomaterials* **2005,***26* (30), 6054-6067.
13. Tsukuda, Y.; Onodera, T.; Ito, M.; Izumisawa, Y.; Kasahara, Y.; Igarashi, T.; Ohzawa, N.; Todoh, M.; Tadano, S.; Iwasaki, N. Therapeutic effects of intra-articular ultra-purified low endotoxin alginate administration on an experimental canine osteoarthritis model. *Journal of Biomedical Materials Research Part A* **2015,***103* (11), 3441-3448.
14. Kim, G. O.; Kim, N.; Kim, D. Y.; Kwon, J. S.; Min, B.-H. An electrostatically crosslinked chitosan hydrogel as a drug carrier. *Molecules* **2012,***17* (12), 13704-13711.
15. Salem, A. K.; Rose, F. R.; Oreffo, R. O.; Yang, X.; Davies, M. C.; Mitchell, J. R.; Roberts, C. J.; Stolnik-Trenkic, S.; Tendler, S. J.; Williams, P. M. Porous polymer and cell composites that self-assemble in situ. *Adv. Mater.* **2003,***15* (3), 210-213.
16. Miyata, T.; Asami, N.; Uragami, T. Preparation of an antigen-sensitive hydrogel using antigen-antibody bindings. *Macromolecules* **1999,***32* (6), 2082-2084.

17. Sant, S.; Coutinho, D. F.; Sadr, N.; Reis, R. L.; Khademhosseini, A. Tissue Analogs by the Assembly of Engineered Hydrogel Blocks. *Biomimetic Approaches for Biomaterials Development* **2012**, 471-493.
18. Whitesides, G. M.; Boncheva, M. Beyond molecules: Self-assembly of mesoscopic and macroscopic components. *Proceedings of the National Academy of Sciences* **2002,***99* (8), 4769-4774.
19. Cheng, H.-w.; Luk, K. D. K.; Cheung, K. M. C.; Chan, B. P. In vitro generation of an osteochondral interface from mesenchymal stem cell–collagen microspheres. *Biomaterials* **2011,***32* (6), 1526-1535.
20. Tan, W.; Desai, T. A. Layer-by-layer microfluidics for biomimetic three-dimensional structures. *Biomaterials* **2004,***25* (7–8), 1355-1364.
21. McGuigan, A. P.; Sefton, M. V. Vascularized organoid engineered by modular assembly enables blood perfusion. *Proceedings of the National Academy of Sciences* **2006,***103* (31), 11461-11466.
22. Chung, S. E.; Park, W.; Shin, S.; Lee, S. A.; Kwon, S. Guided and fluidic self-assembly of microstructures using railed microfluidic channels. *Nature materials* **2008,***7* (7), 581-587.
23. Du, Y.; Lo, E.; Ali, S.; Khademhosseini, A. Directed assembly of cell-laden microgels for fabrication of 3D tissue constructs. *Proceedings of the National Academy of Sciences of the United States of America* **2008,***105* (28), 9522-9527.
24. Fernandez, J. G.; Khademhosseini, A. Micro-masonry: construction of 3D structures by microscale self-assembly. *Adv. Mater.* **2010,***22* (23), 2538-2541.
25. Xu, M.; Wang, X.; Yan, Y.; Yao, R.; Ge, Y. An cell-assembly derived physiological 3D model of the metabolic syndrome, based on adipose-derived stromal cells and a gelatin/alginate/fibrinogen matrix. *Biomaterials* **2010,***31* (14), 3868-3877.
26. Ekici, S.; Ilgin, P.; Yilmaz, S.; Aktas, N.; Sahiner, N. Temperature and magnetic field responsive hyaluronic acid particles with tunable physical and chemical properties. *Appl. Surf. Sci.* **2011,***257* (7), 2669-2676.
27. Liu, B.; Liu, Y.; Lewis, A. K.; Shen, W. Modularly assembled porous cell-laden hydrogels. *Biomaterials* **2010,***31* (18), 4918-4925.
28. Harada, A.; Kobayashi, R.; Takashima, Y.; Hashidzume, A.; Yamaguchi, H. Macroscopic self-assembly through molecular recognition. *Nature chemistry* **2011,***3* (1), 34-37.
29. Yamaguchi, H.; Kobayashi, Y.; Kobayashi, R.; Takashima, Y.; Hashidzume, A.; Harada, A. Photoswitchable gel assembly based on molecular recognition. *Nature communications* **2012,***3*, 603.
30. Qi, H.; Ghodousi, M.; Du, Y.; Grun, C.; Bae, H.; Yin, P.; Khademhosseini, A. DNA-directed self-assembly of shape-controlled hydrogels. *Nature communications* **2013,***4*.
31. Gillette, B. M.; Jensen, J. A.; Tang, B.; Yang, G. J.; Bazargan-Lari, A.; Zhong, M.; Sia, S. K. In situ collagen assembly for integrating microfabricated three-dimensional cell-seeded matrices. *Nature materials* **2008,***7* (8), 636-640.
32. Yu, Y.; Kieviet, B. D.; Kutnyanszky, E.; Vancso, G. J.; de Beer, S. Cosolvency-induced switching of the adhesion between poly (methyl methacrylate) brushes. *ACS macro letters* **2014,***4* (1), 75-79.
33. Cao, Z.; Dobrynin, A. V. Nanoparticles as Adhesives for Soft Polymeric Materials. *Macromolecules* **2016,***49* (9), 3586-3592.
34. Rose, S.; Prevoteau, A.; Elzière, P.; Hourdet, D.; Marcellan, A.; Leibler, L. Nanoparticle solutions as adhesives for gels and biological tissues. *Nature* **2014,***505* (7483), 382-385.
35. Brunel, B.; Beaune, G.; Nagarajan, U.; Dufour, S.; Brochard-Wyart, F.; Winnik, F. M. Nanostickers for cells: a model study using cell–nanoparticle hybrid aggregates. *Soft Matter* **2016,***12* (38), 7902-7907.
36. Mero, A.; Campisi, M. Hyaluronic acid bioconjugates for the delivery of bioactive molecules. *Polymers* **2014,***6* (2), 346-369.
37. Demadis, K. D.; Paspalaki, M.; Theodorou, J. Controlled release of bis (phosphonate) pharmaceuticals from cationic biodegradable polymeric matrices. *Industrial & Engineering Chemistry Research* **2011,***50* (9), 5873-5876.

38. Fuller, K.; Tabor, D. In *The effect of surface roughness on the adhesion of elastic solids*, Proceedings of the Royal Society of London A: Mathematical, Physical and Engineering Sciences, 1975; The Royal Society, pp 327-342.
39. Izumrudov, V. A.; Kharlampieva, E.; Sukhishvili, S. A. Multilayers of a globular protein and a weak polyacid: role of polyacid ionization in growth and decomposition in salt solutions. *Biomacromolecules* **2005,***6* (3), 1782-1788.

TOC Graphic